International Journal of Earthquake Engineering – IJE
Volume 1: Issue 1 [ISSN 2475-2754]
Publication Date : 09 January 2014

# Adaptive control of base-isolated Structures against near-field Earthquakes using MR damper

Peyman Safapour [a,1] , Hossein A. Rahimi [a] , Mansour Rafeeian [b]

[a] Department of Civil Engineering, Yazd University, Iran

[b] Department of Mechanical Engineering, Yazd University, Iran

ABSTRACT

Magnetorheological (MR) dampers are semi-active devices that can be used to control the response of structures during seismic loads. They have the adaptability of active devices and stability and reliability of passive devices. One of the challenges in the application of the MR dampers is to develop an effective strategy of control that can fully exploit the capabilities of the MR dampers. This paper investigates the effectiveness of an adaptive strategy of control for modulating the command voltage of Magnetorheological dampers which are employed as semi-active devices in combination with laminated rubber bearings for the seismic protection of buildings. The controller developed in this study is an adaptive fuzzy neural controller (AFNC). It consists of a direct fuzzy controller with self-tuning scaling factors based on neural networks. A simple feed forward neural network is implemented to adjust the input scaling factors such that the fuzzy controller effectively determines the command voltage of the damper according to the current level of ground motion. For the purpose of comparison, a passive operation is also considered in simulating maximum voltage operation of MR damper. The results reveal that the developed adaptive controller can successfully improve the seismic response of base-isolated buildings against various types of earthquake.

## 1. Introduction

Mitigation for dynamic responses of structures induced by severe dynamic loads, such as earthquake and strong wind, is a challenging topic [1]. Over past decades, base isolation has been found to be an effective way to keep structures and their contents safe from the destructive effects of dynamic excitations. However, recent studies have shown that near-field earthquakes characterized by long-duration pulses with peak velocities result in significant relative displacements at the isolation level of a seismically isolated structure [2–4]. As a result of large isolator displacements, the size of the isolation device significantly increases. This may require very large seismic gaps between buildings or large bridge expansion joints [5]. Therefore, these requirements, in return increase the cost of the construction, which contradicts the primary goal of seismic isolation to design buildings more efficiently and economically by reducing the earthquake forces transferred to the superstructure. In order to improve the performance of base-isolated structures, passive, active, and semi-active control devices have been proposed [6–12]. Passive systems which require no external energy, can reduce the isolation bearings displacements during strong ground motions; however, they can cause an increase in superstructure response due to large damper forces applied to the structure [13–15]. Furthermore, in the case of a moderate or weak excitation, passive devices can have negative effects on an isolated structure since the desired isolation characteristics may be different for these ground motions and passive devices cannot be adapted online [5]. These devices are reliable and never destabilize the structure. On the other hand, active devices are generally adaptive to varying usage patterns and loading conditions and they can control the seismic response of the isolation system for a wide range of loading conditions. However, active devices use an external power source to produce the control forces imparted on the structure and they require a considerable size of power source, which makes them at the risk of power failure. Also, an active control system has the potential to destabilize the structural system. Recently, semi-active control devices have attracted a great deal of attention in civil engineering field, because they offer the adaptability of active control devices without requiring

[1] corresponding author Tel: +98 913319 5295

*E-mail address:* peyman.safapour@gmail.com

large power sources [16]. These devices only absorb or store the vibratory energy and they do not input the energy to the system. Therefore, they do not induce detrimental effects on the stability of the system [17]. Several researchers have studied the use of a semi-active device in a base isolation system in order to reduce the displacement response of an isolation system without an increase in superstructure response. Yoshioka et al. [18] performed experimental tests to find the effectiveness of a base isolation system that employs a magnetorheological (MR) damper. Symans and Kelly [19] investigated the performance of a variable viscous damper adjusted by a fuzzy controller for the seismic protection of an isolated bridge. In another experiment, Nagarajaiah and Sahasrabudhe [20] proposed a variable stiffness device that is used in a sliding isolation system to reduce the seismic response of a base-isolated building, and the effectiveness of the proposed semi-active device was shown by performing analytical and experimental studies. Madhekar and Jangid [21] evaluated the dynamic response of a seismically isolated benchmark bridge equipped with viscous and variable dampers and assessed the performance of such dampers. One semi-active device that appears to be promising for structural control applications is the magnetorheological damper. This is a new kind of semi-active control device, which utilizes the essential characteristic of MR fluids being their ability to reversibly change from free-flowing, linear viscous liquids to semi-solids having controllable yield strength in milliseconds when exposed to magnetic field. At the same time it has merits of simple construction, cheap cost, insensitiveness to temperature and excellent control effect, thereby gaining more attention. MR dampers are usually installed on the deformation position, such as the braces between columns or between ground and foundation. When structures deform due to vibration, MR dampers will adjust their characteristic in accordance with given situation and will absorb vibration energy. One of the challenges in the application of the MR dampers is using an appropriate control algorithm to compute the command voltage of the MR damper, quickly and precisely. As is the case for other passive devices, passive control of MR damper cannot adjust the generated force in real time according to the structural responses. When the force is chosen very large, the damper will increase superstructure forces due to moderate and weak ground motions. On the other hand, when the force is chosen not big enough, the damper will have small energy dissipation capacity under strong earthquakes due to its small force [5]. Therefore, a controllable generating force is essential in order to ensure the required amount of energy dissipation for various levels of ground motion. In order to utilize the full capabilities of a MR damper employed in a smart isolation system, an effective control algorithm that is practically viable is needed. However, the task of developing an optimal controller is challenging due to uncertainties in the nature of ground motions and in the characteristics of isolation system. For instance, a controller designed for near-field ground motions that cause significant deformations in the isolation system might develop large damper forces during a far-field earthquake of generally more moderate excitation. As a result, the isolation system may not perform as expected, and a significant increase in the acceleration response of superstructure can be observed. Alternatively, if the controller is designed for an earthquake with far field characteristics, the damper force may not be large enough to effectively dissipate the motion during a pulse like ground motion [5]. Many control algorithms have been proposed to control the behavior of MR dampers or other semi-active devices. Decentralized bang–bang control [22], the methods based on the Lyapunov theory to minimize the rate of change of a Lyapunov function [23] or to decrease the total energy of the structure [24], clipped-optimal control [25] and modulated homogeneous friction control [26] are some of the control algorithms used for semi-active control devices. Each of these control strategies has its own merits and limitations depending on the situation and desired response, and comparative studies are needed to evaluate the performance of each control method.

In this study, an adaptive control strategy is developed in order to adjust the controllable force of the MR dampers (MRs) that are used in a smart isolated system. The controller is based on an intelligent strategy of control. In particular, fuzzy logic theory of control is used to design an adaptive controller whose input scaling factors are tuned by a simple neural network according to the current level of ground motion. The adaptive fuzzy neural controller (AFNC) determines the command voltage by using isolation displacement and velocity as the two input variables. A five-story building isolated by laminated rubber bearings is modeled together with magnetorheological dampers which are installed to the base of the building. Numerical simulations of the base-isolated building are performed and various response quantities are evaluated in order to assess the performance of the controllers.

## 2. Modeling of a base-isolated structure with MR dampers

Consider an n degree of freedom linear base-isolated structure subject to earthquake ground acceleration $\ddot{x}_g$. The equation governing the dynamic response of the structural system equipped with MR dampers located at certain levels of the structure is given by

$$\mathbf{M}\ddot{\mathbf{x}}(\mathrm{t}) + \mathbf{C}\dot{\mathbf{x}}(\mathrm{t}) + \mathbf{K}\mathbf{x}(\mathrm{t}) = -\mathbf{M}\mathbf{I}\ddot{\mathbf{x}}_{\mathbf{g}}(\mathrm{t}) + \mathbf{D}\mathbf{u}(\mathrm{t}) \qquad (1)$$

Where **M**, **C**, and **K** denotes n×n mass, damping, and stiffness matrices, respectively; **D** is an n×1 damper location vector; **I** is an n-dimensional identity matrix; **x**(t), $\dot{\boldsymbol{x}}(t)$, and $\ddot{\boldsymbol{x}}(t)$ are n×1 displacement, velocity, and acceleration vectors, respectively; and **u**(t) is an n×1 control force vector.
Rewriting Eq. (1) in state-space form gives

$$\dot{\boldsymbol{z}}(\boldsymbol{t}) = \boldsymbol{A}\boldsymbol{z}(t) + \boldsymbol{B}\boldsymbol{f}(t) \quad (2)$$
$$\boldsymbol{y}(t) = \boldsymbol{C}\boldsymbol{z}(t) + \boldsymbol{D}\boldsymbol{f}(t) \quad (3)$$

where $\boldsymbol{z}(t) = [\boldsymbol{x}(t), \dot{\boldsymbol{x}}(t)]^T$ denotes the state vector of the system. Also, the system parameters **A**, **B,** **C** and **D** are defines as follows:

$$\boldsymbol{A}_{2n\times 2n} = \begin{bmatrix} \boldsymbol{0} & \boldsymbol{I} \\ -\boldsymbol{M}^{-1}\boldsymbol{K} & -\boldsymbol{M}^{-1}C \end{bmatrix} \quad \boldsymbol{C}_{2n\times 2n} = \begin{bmatrix} \boldsymbol{0} & \boldsymbol{H} \\ \boldsymbol{H} & \boldsymbol{0} \end{bmatrix}$$
$$\boldsymbol{B}_{2n\times m} = \begin{bmatrix} \boldsymbol{0}_{6\times 1} & \boldsymbol{0}_{6\times 6} \\ -\boldsymbol{r}_{6\times 1} & \boldsymbol{M}^{-1} \end{bmatrix} \quad \mathbf{D} = \mathbf{0} \quad (4)$$

**H** is an n×n matrix, whose diagonal arrays are 1 and the rest of arrays are equal to zero.

### 2.1. Dynamic model of MR damper

In this study, the phenomenological model of a MR damper is used to model the dynamic behavior of the dampers. The mechanical model for MR damper based on the Bouc–Wen hysteresis model is shown in Fig. 1. The force f generated by the MR damper is calculated by [27]

$$f = c_1\dot{y} + k_1(x - x_0) \quad (5)$$

$$\dot{z} = -\gamma|\dot{x} - \dot{y}|z|z|^{n-1} - \beta(\dot{x} - \dot{y})|z|^n + A(\dot{x} - \dot{y}) \quad (6)$$

$$\dot{y} = (1/(c_0 + c_1))\{\alpha z + c_0\dot{x} + k_0(x - y)\} \quad (7)$$

Where $\dot{x}$ and $c_0$ are velocity and viscous damping of the MR damper, and z is the evolutionary variable. As shown in Eq. (6), the hysteresis behavior of MR damper is expressed by a first-order differential equation. The variables γ, β, n, $k_0$, $x_0$ and A are adjustable shape parameters of the hysteresis loops for the yielding element in the MR damper [27]. These variables can control the linearity in the unloading and the smoothness of the transition from the pre-yield to the post-yield region. Parameters of the model of MR damper governing equation α and $c_0$ are the functions of the applied voltage *v* as follows

$$\alpha = \alpha_a + \alpha_b u \quad (8)$$

$$c_0(u) = c_{0a} + c_{0b}u \quad (9)$$

$$c_1(u) = c_{1a} + c_{1b}u \quad (10)$$

$$\dot{u} = -\eta(u - v) \quad (11)$$

where *u* and *v* are the input and output voltages and η is the constant time of the first-order filter. The variables $\alpha_a$, $\alpha_b$, $c_{0a}$ and $c_{0b}$ are parameters that account for the dependence of the MR damper force on voltages applied to the current driver and the resulting magnetic current [27].

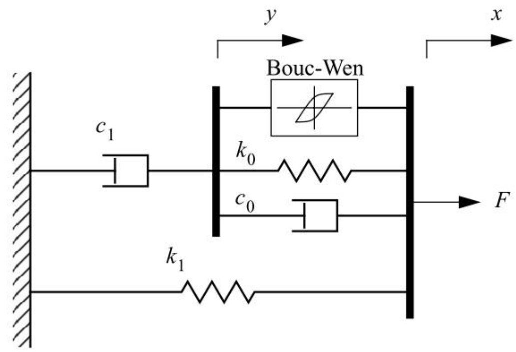


**Fig. 1.** Phenomenological model of MR damper

Note that unlike the active devices, semi-active devices can produce dissipative forces only in the same direction with the velocity of the damper. In addition, there is an upper and lower limit on the force produced by the MR damper which depends on damper velocity at any considered time [17].

### 3. Adaptive fuzzy neural control strategy

Adaptive control is a method by which a controller is designed to have the capability of tuning its parameters automatically [5]. The primary goal of using adaptive controllers is to improve the performance of the controller online in the face of changing uncertain parameters. This section introduces adaptive fuzzy neural controller that is designed to adjust the generate force of MR dampers according to the current level of external excitation.

Fuzzy logic control is an effective approach which offers a simple and robust framework to deal with uncertainties and complex nonlinear systems. Fuzzy logic enables one to describe relationships between the inputs and outputs of a controller using simple verbose statements instead of complicated mathematical terms. Due to its inherent robustness and simplicity, several researchers have used fuzzy logic theory to develop controllers for semi-active devices [28–30]. The design of a fuzzy logic controller (FLC) involves several steps. The first step is fuzzification, which is the process of converting crisp values to linguistic fuzzy values by assigning membership functions to each input and output variable. The next step is decision making, which involves evaluation of a series of if–then rules. In this step, a fuzzy rule base is created to relate the inputs and outputs. The third step is the definition of an inference engine that evaluates the rules to produce the system output, and by Using a fuzzy inference mechanism, the rules are evaluated to specify the output for a given input set. The final step, defuzzification, is to transform the output variable that is a fuzzy quantity to a non-fuzzy discrete value [5,17]. The performance of a conventional FLC depends on various controller parameters such as the scaling

**Table 1**
Characteristics of the ground motions used in the analyses.

| Record (Station & Direction ) | Earthquake | Magnitude (Mw) | Peak Ground acceleration (g) | Peak ground velocity (cm/s) | Source of data |
|---|---|---|---|---|---|
| El centro 270° | 1940 El Centro | 7.2 | 0.32 | 36.3 | USGS[1] |
| Pacoima Dam 254° | 1971 San Fernando | 6.6 | 1.16 | 54.3 | CDMG[2] |
| Hollister-South & Pine 0° | 1989 Loma Prieta | 6.9 | 0.37 | 62.4 | CDMG |
| Sylmar-Olive View Med FF 360° | 1994 Northridge | 6.7 | 0.84 | 129.6 | CDMG |
| Takarazuka 0° | 1995 Kobe | 6.9 | 0.693 | 68.3 | CDMG |
| TCU068 N-S | 1999 Chi-Chi | 7.6 | 0.462 | 263.2 | CWB[3] |

[1] http://nsmp.wr.usgs.gov/ [2] http://docinet3.consrv.ca.gov/csmip/ [3] http://www.cwb.gov.tw/

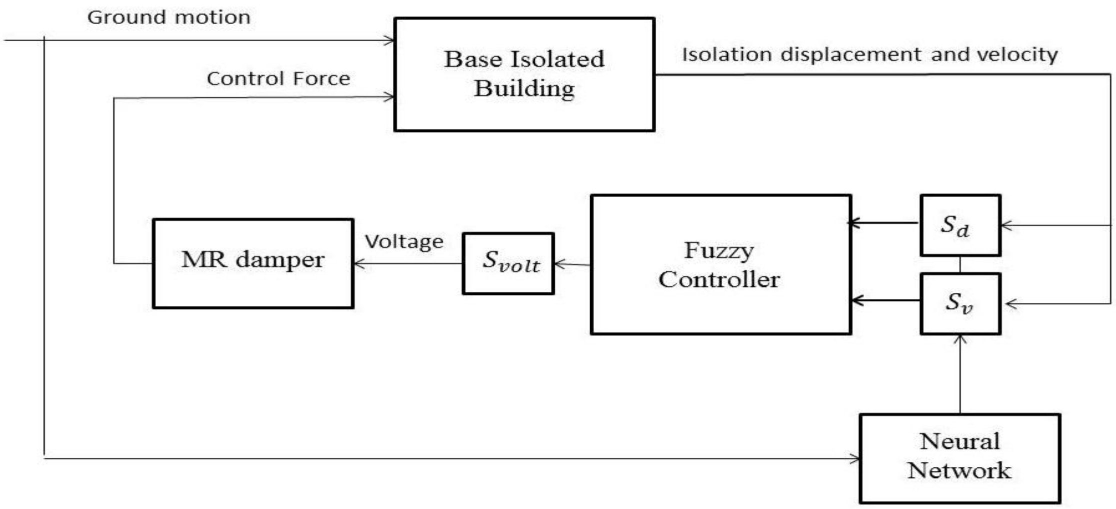


**Fig. 2.** Block diagram of the adaptive fuzzy neural controller

factors, membership functions, and rule base. In order to improve the effectiveness of the controller, an adaptive FLC can be designed by varying each of these parameters. Here, neural networks, are employed to tune the input scaling factors of a fuzzy controller to ensure acceptable controller performance for both near-field and far-field ground motions. By modifying the scaling factors of input variables, the corresponding universe of discourse of the variable will enlarge or reduce, resulting in better performance of the fuzzy controller. The block diagram of the adaptive fuzzy neural controller is shown in Fig. 2

The mamdani fuzzy logic controller developed in this study employs isolation system displacement and velocity as two input variables and provides the command voltage of the damper. Seven triangular membership functions are defined for each input variable, as shown in Fig. 3. The fuzzy sets for the input variables are NL = negative large, NM = negative medium, NS = negative small, ZE = zero, PS = positive small, PM = positive medium, and PL =positive large. Note that the universe of discourse for each input variable is defined from -1 to 1. scaling factor should be selected because, if the inputs are scaled to the values such that they become too small, then the innermost membership functions will be used frequently. On the other hand, if they become too big after being scaled, then the outermost membership function will be mostly employed, and this limits the perfirmance of the controller. Since the amplitudes of isolation deformation and velocity differ greatly for near-field and far-field ground motions, the decision on the scaling factors is done by a simple feedforward neural network, introduced later in this section.

Five triangular membership functions are defined to cover the universe of discourse of the output variable voltage. The maximum driving voltage for the MR damper is 3V. However, if the damper is operated at its full capacity during a far-field earthquake, the generated force of the damper will be too large and the damper will increase superstructures acceleration. The output membership functions are equally spaced over the output domain, as shown in Fig. 4. The fuzzy sets for the output variables are VL =very large, L =large, M =medium, S =small, and ZE =zero.

After the fuzzification of the input and output variables, a fuzzy rule base is defined for the FLC. The rule bases adopted for the

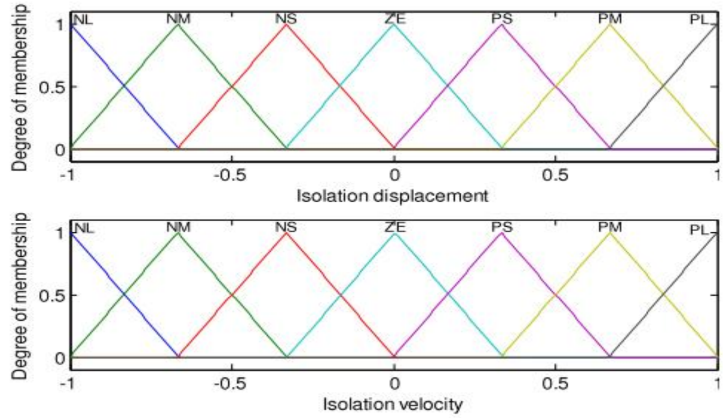


**Fig. 3.** Input membership functions

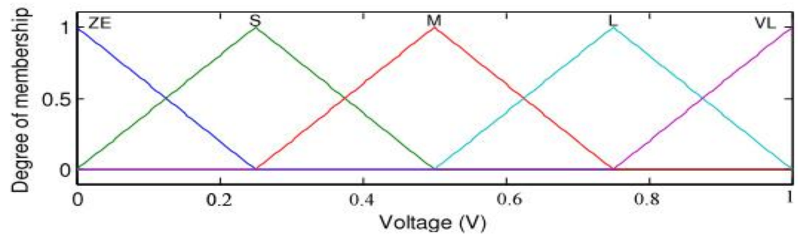


**Fig. 4.** Output membership function

developed fuzzy controller are given in Table 2. The control rules are in the form of if–then statements, and they map the link between the input and output membership functions. Since the rules are words instead of mathematical equations, it is easy to interpret and modify the rules

The rationale for forming the rule bases is as follows: if the displacement and velocity of the isolation system is of opposite sign, then the output voltage is small, and if the isolation displacement and velocity have the same sign, then the output voltage is large. The magnitude of the output is linearly proportional to the magnitude of the input variables. When the displacement and velocity are almost zero or small, the command voltage is about zero; The center of area method is used as a defuzzification method for the FLC to get a crisp output value.

Neural networks have been used widely used for adaptive control of uncertain systems [31]. An artificial neural network consists of simple artificial neurons that are usually organized into three layers, namely, an input layer, a hidden layer, and an output layer, with random connections between the layers. The input signals, are modified by synaptic weights. The output of a neuron is specified by an activation function whose input is the sum of weighted inputs.

A simple 2 layer neural network that consists of five artificial neurons in the hidden layers and trained with levenberg-Marquardt algorithm is constructed to specify the input scaling factors of the fuzzy controller. As discussed earlier, near-field earthquakes usually possess long duration pulses with peak veloc--ities. Therefore, the ground velocity $\dot{x}_g$ is selected as the input of each neuron in order to determine the characteristics of the ground motion. The range of the input $\dot{x}_g$ is defined to be [-100 100] cm/s, where the upper limit of |100| cm/s is set as a saturation point and seismic records with ground velocities beyond this value are directly classified as near-field earthquakes [5]. The outputs of the network are scaling factors for the isolation displacement Sd, isolation velocity Sv. The activation functions chosen for the neural network are tangent sigmoidal function in hidden layer and the linear function for the output layer. The pairs used for training the network is built with the trial and error of narasimhan evaluation criteria [32]. For each of these ground motions, the fuzzy controller discussed earlier is made up and with tuning the scaling factors by trial and error the best ones are picked up for training pairs. Because the data was not continuous for all of inputs a linear interpolation used to cover the range.

## 4. Numerical study A five-story base-isolated building, as studied by Johnson et al.

A five-story base-isolated building, as studied by Johnson et al. [32], was selected to investigate the performance of developed adaptive controllers. A lumped-mass structure model with one degree of freedom per floor is used in the numerical simulations. The fundamental period of the building is 0.3 s, with a damping of 2% in the first mode. Structural parameter of the model is shown in Table 3.

In order to improve the performance of the base-isolated building against different earthquakes, 6 MR dampers with a total force capacity of 18 kN are installed in the base of the structure.

Time history analysis of the base-isolated building were per- -formed in MATLAB/Simulink [33] for the six historical earthquakes.

**Table 2**
Fuzzy Rule Base

| | | Isolation displacement | | | | | | |
|---|---|---|---|---|---|---|---|---|
| | **voltage** | **NL** | **NM** | **NS** | **ZE** | **PS** | **PM** | **PL** |
| Isolation velocity | **NL** | VL | VL | L | L | M | S | ZE |
| | **NM** | VL | L | L | M | S | ZE | S |
| | **NS** | L | L | M | S | ZE | S | M |
| | **ZE** | L | M | S | ZE | S | M | L |
| | **PS** | M | S | ZE | S | M | L | L |
| | **PM** | S | ZE | S | M | L | L | VL |
| | **PL** | ZE | S | M | L | L | VL | VL |

The evaluated response parameters are maximum isolator displacement $x_{b,max}$, maximum interstory drift $d_{s,max}$, maximum floor acceleration $\ddot{x}_{s,max}$, and maximum damper force $F_{d,max}$. The results for the base-isolated building without any damper (uncontrolled structure), for the maximum passive operation of the MR dampers, and for the Fixed Base structure, are also given in Table 4 for the purpose of comparison. The minimum value of each response quantity for various controller cases is indicated in bold in the table.

It can be seen that passive operation of MRs with maximum voltage significantly reduces the peak isolation deformation for all considered excitations without any increase in interstory drifts, except in the case of the San Fernando earthquake. Specifically, the reduction of the maximum base displacement is of the order of 17% to 50%. However, there is an amplification for the maximum floor acceleration for most of the cases. In particular, the maximum floor acceleration increases by 268%, 36%, and 6% for the San Fernando, Kobe, and Loma Prieta earthquakes, respectively.

The semi-active control of MRs, efficiently improves the performance of base-isolated building concerning the peak acceleration response at the cost of slight deterioration in the peak isolation deformation. When the performances of two control strategies are compared, it can be seen that developed adaptive control method is more effective than a Passive max, controller, especially in controlling the acceleration response of the base-isolated building. The increases in floor acceleration are only 54%, 4%, for the AFNC for the San Fernando and Kobe earthquakes respectively. when the performances of the AFNC, Passive max and uncontrolled isolated structure is compared with fixed base structure, it can be observed that the acceleration and story drifts for all of cases are much lesser than a fixed base structure.

Figs. 5 and 6 show the time histories of the isolator displacement and top floor acceleration for the semi-active control of the base-isolated building with the AFNC, Passive Max and Fixed Base structure subjected to the El Centro and Chi-Chi earthquakes, respectively. The results of the uncontrolled structure are also provided as a measure of performance evaluation of semi-active controllers. Also, a force–displacement diagram of the MRs and the time history of the command voltage for the AFNC presented in Figs.7 for the Northridge excitation case.

There are different sets of evaluation criteria which are used in the benchmark problem in structural control to evaluate the performance of the buildings [32]. For better evaluating the proposed control method, the set of evaluation criteria used in this study to compare the performance of the structure controlled with different methods is listed below

$$J_1(q) = \frac{max_t \|V_0(t,q)\|}{max_t \|\hat{V}_0(t,q)\|} \tag{12}$$

$$J_2(q) = \frac{max_{t,i} \|d_i(t,q)\|}{max_{t,i} \|\hat{d}_i(t,q)\|} \tag{13}$$

$$J_3(q) = \frac{max_{t,f} \|d_f(t,q)\|}{max_{t,f} \|\hat{d}_f(t,q)\|} \tag{14}$$

$$J_4(q) = \frac{max_{t,f} \|a_f(t,q)\|}{max_{t,f} \|\hat{a}_f(t,q)\|} \tag{15}$$

Where $V_0(t,q)$, $d_i(t,q)$, $d_f(t,q)$, $a_f(t,q)$ are maximum base shear, maximum base drift, maximum story drifts and maximum story acceleration of controlled structure, respectively. The variables $\hat{V}_0(t,q)$, $\hat{d}_i(t,q)$, $\hat{d}_f(t,q)$ and $\hat{a}_f(t,q)$ are the maximum base shear, maximum base drift, maximum story drifts and maximum story acceleration of the uncontrolled structure, respectively. The data are listed in table 5 for San Fernando and ChiChi earthquakes.

## 5. Conclusions

The aim of this study was to investigate the effectiveness of an adaptive control strategy that were employed to modulate the generate force of magnetorheological dampers installed in a base-isolated building. The developed adaptive controller goal is to reduce the isolation system deformations without increasing the

**Table 4**

Maximum responses of the base-isolated structure for several seismic excitations.

| Earthquake | Response | Uncontrolled | Fixed Base | AFNC | Passive-Max |
|---|---|---|---|---|---|
| Elcentro | $x_{b,max}$ | 39.43 | -- | 21.64 | **19.40** |
| | $d_{s,max}$ | 0.22 | 1.05 | **0.14** | 0.16 |
| | $\ddot{x}_{s,max}$ | 2.55 | 16.26 | **1.95** | 2.06 |
| | $F_{d,max}$ | -- | -- | 18.00 | 18.00 |
| San Fernando | $x_{b,max}$ | 15.36 | -- | 9.86 | **8.53** |
| | $d_{s,max}$ | 0.12 | 1.62 | **0.10** | 0.15 |
| | $\ddot{x}_{s,max}$ | **1.06** | 24.90 | 1.63 | 3.91 |
| | $F_{d,max}$ | -- | -- | **15.86** | 18.00 |
| Loma Prieta | $x_{b,max}$ | 35.76 | -- | 27.48 | **25.01** |
| | $d_{s,max}$ | 0.20 | 0.89 | **0.19** | **0.19** |
| | $\ddot{x}_{s,max}$ | 2.36 | 13.25 | **2.34** | 2.51 |
| | $F_{d,max}$ | -- | -- | 18.00 | 18.00 |
| Northridge | $x_{b,max}$ | 145.73 | -- | 122.85 | **120.70** |
| | $d_{s,max}$ | 0.82 | 1.17 | **0.67** | 0.73 |
| | $\ddot{x}_{s,max}$ | 9.48 | 16.98 | 8.56 | **8.44** |
| | $F_{d,max}$ | -- | -- | 18.00 | 18.00 |
| Kobe | $x_{b,max}$ | 38.82 | -- | 31.22 | **26.77** |
| | $d_{s,max}$ | 0.22 | 0.63 | 0.22 | **0.20** |
| | $\ddot{x}_{s,max}$ | **2.57** | 12.35 | 2.67 | 3.50 |
| | $F_{d,max}$ | -- | -- | 18.00 | 18.00 |
| Chi-Chi | $x_{b,max}$ | 59.44 | -- | 39.51 | **36.43** |
| | $d_{s,max}$ | 0.33 | 0.67 | **0.21** | 0.25 |
| | $\ddot{x}_{s,max}$ | 3.84 | 12.34 | **2.81** | 3.01 |
| | $F_{d,max}$ | -- | -- | 18.00 | 18.00 |

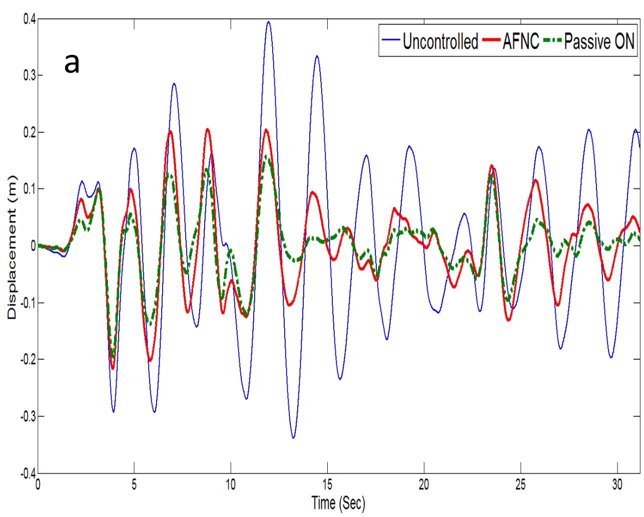


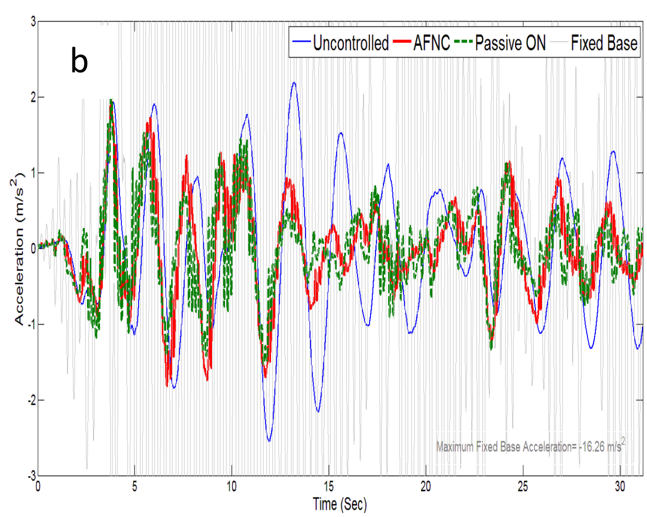


**Fig. 5.** Time histories of (a) isolator displacement and (b) top floor acceleration subjected to the Elcentro earthquake.

superstructure accelerations significantly during dynamic excitations. The controller is an adaptive fuzzy neural controller that has an online tunable input universe of discourse in order to determine the command voltage of the damper according to current level of ground motion. Maximum passive operation of the MRs and fixed base structure, was also considered in order to evaluate the performance of the adaptive controllers. The results from numerical simulations with several ground motions demons-

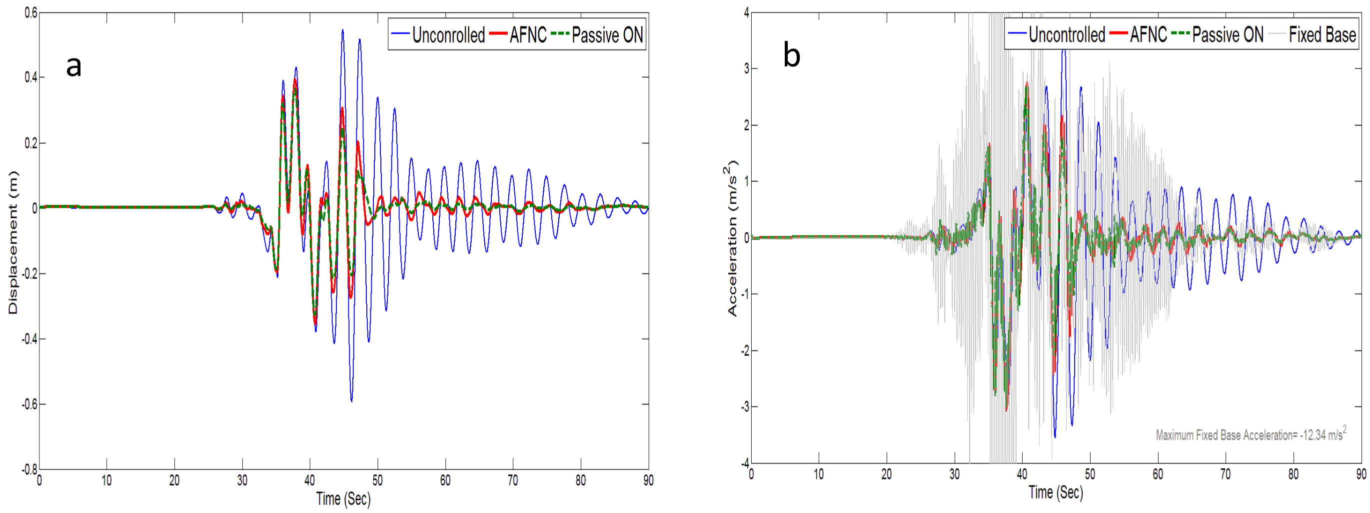


**Fig. 6.** Time histories of (a) isolator displacement and (b) top floor acceleration subjected to the Chi-Chi earthquake.

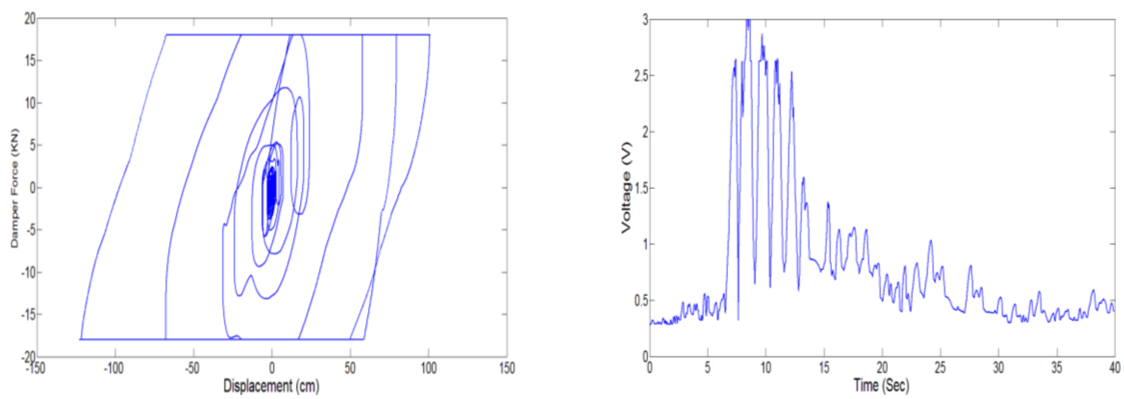


**Fig. 7.** Force-displacement diagram of MRs and time history of the command voltage for base-isolated structure subjected to the Northridge

**Table 5**

Evaluated performance indices due to (Left) Chi-Chi and (Right) San Fernando Earthquakes.

| Uncontrolled | Passive-Max | AFNC | Criteria | Uncontrolled | Passive-Max | AFNC | Criteria |
|---|---|---|---|---|---|---|---|
| 1.620 | 0.714 | 0.609 | $J_1$ | 4.171 | 0.704 | 0.280 | $J_1$ |
| - | 0.613 | 0.665 | $J_2$ | - | 0.554 | 0.642 | $J_2$ |
| 2.012 | 0.740 | 0.629 | $J_3$ | 2.030 | 0.875 | 0.125 | $J_3$ |
| 3.214 | 0.784 | 0.732 | $J_4$ | 23.491 | 3.689 | 1.538 | $J_4$ |
| - | 0.051 | 0.051 | $J_5$ | - | 0.051 | 0.0446 | $J_5$ |

-trate that MR dampers that operate as semi-active devices by employing adaptive control strategy developed in this study can effectively improve the response of base-isolated buildings against both far-field and near-field ground motions.

**Table 3**
Structural model parameters (Kelley et al, 1987)

| Floor Masses [kg] | Stiffness Coefficients [KN/m] | Damping Coefficients [KNs/m] |
|---|---|---|
| $m_0$ = 6800 | $K_0$ = 232 | $C_0$ = 7.45 |
| $m_1$ = 5897 | $K_1$ = 33732 | $C_0$ = 67 |
| $m_2$ = 5897 | $K_2$ = 29093 | $C_0$ = 58 |
| $m_3$ = 5897 | $K_3$ = 28621 | $C_0$ = 57 |
| $m_4$ = 5897 | $K_4$ = 24954 | $C_0$ = 50 |
| $m_5$ = 5897 | $K_5$ = 19059 | $C_0$ = 38 |

**References**

[1] Xu ZD, Guo YQ. Fuzzy control strategy for earthquake-excited nonlinear magnetorheological structures. Soil Dyn and Earth Eng 2001;28:717-727.

[2] Jangid RS, Kelly JM. Base isolation for near-fault motions. Earthq Eng Struct Dyn 2001;30:691–707.

[3] Shen J, Tsai MH, Chang KC, Lee GC. Performance of a seismically isolated bridge under near-fault earthquake ground motions. J Struct Eng 2004;130(6):861–8.

[4] Heaton TH, Hall JF, Wald DJ, Halling MV. Response of high-rise and base isolated buildings to a hypothetical Mw 7 blind thrust earthquake. Science 1995;267:206–11.

[5] Ozbulut OE, Bitaraf M, Hurlebaus S. Adaptive control of base-isolated structures against near-field earthquakes using variable friction dampers. Eng Struct 2011;33:3143-3154.

[6] Dicleli M. Supplemental elastic stiffness to reduce isolator displacements for seismic-isolated bridges in near-fault zones. Eng Struct 2007;29:763–75.

[7] Barbat AH, Rodellar J, Ryan EP, Molinares N. Active control of nonlinear base-isolated buildings. J Eng Mech 1995;121(6):676–85.

[8] Ozbulut OE, Hurlebaus S. Optimal design of superelastic-friction base isolators for seismic protection of highway bridges against near-field earthquakes. Earthq Eng Struct Dyn 2011;40:273–91

[9] Bitaraf M, Barroso LR, Hurlebaus S. Adaptive control to mitigate damage impact on structural response. J Intell Mater Syst Struct 2010;21:607–19. doi:10.1177/1045389X10361993.

[10] Nagarajaiah S, Narasimhan S. Seismic control of smart base isolated building with new semi-active variable damper. Earthq Eng Struct Dyn 2007;36: 729749.

[11] Shook DA, Roschke PN, Ozbulut OE. Superelastic semi-active damping of a base-isolated structure. Struct Control Health Monitoring 2008;15:746–68.

[12] Hurlebaus S, Gaul L. Smart structure dynamics. Mech Syst Signal Process 2006;20:255–81.

[13] Kelly JM. Role of damping in seismic isolation. Earthq Eng Struct Dyn 1999; 28(1):3–20.

[14] Mazza F, Vulcano A. Nonlinear response of RC framed buildings with isolation and supplemental damping at the base subjected to near-fault earthquakes. J Earthq Eng 2009;13:690–715.

[15] Alhan C, Gavin H. A parametric study of linear and non-linear passively damped seismic isolation systems for buildings. Eng Struct 2004;26(4): 485–97.

[16] Gaul L, Hurlebaus S, Wirnitzer J, Albrecht H. Enhanced damping of lightweight structures by semi-active joints. Acta Mech 2008;195:249–61.

[17] Bitaraf M, Ozbulut OE, Hurlebaus S, Barroso L. Application of semi-active control strategies for seismic protection of buildings with MR dampers. Eng Struct 2010;32:3040-3047.

[18] Yoshioka H, Ramallo JC, Spencer BF. Smart base isolation strategies employing magnetorheological dampers. J Eng Mech 2002;128(5):540–51.

[19] SymansMD,KellySW.Fuzzy logic control of bridge structures using intelligent semi-active seismic isolation systems. Earthq Eng Struct Dyn 1999;28:37–60.

[20] Nagarajaiah S, Sahasrabudhe S. Seismic response control of smart sliding isolated buildings using variable stiffness systems: an experimental and numerical study. Earthq Eng Struct Dyn 2006;35(2):177–97.

[21] Madhekar SN, Jangid RS. Variable dampers for earthquake protection of benchmark highway bridges. Smart Mater Struct 2009;18:1–18.

[22] Feng Q, Shinozuka M. Use of a variable damper for hybrid control of bridge response under earthquake. In: US national workshop on structural control researh 1990. Los Angeles: University of Southern California; p. 107–12.

[23] Brogan WL. Modern control theory. Englewood Cliffs (NJ): Prentice-Hall; 1991.

[24] McClamroch NH, Gavin HP. Closed loop structural control using electrorheological dampers. In: American control conference. Washington (DC): American Automatic Control Council; 1995.

[25] Dyke SJ, Spencer BF. Seismic response control using multiple MR dampers. In: 2nd international workshop on structural control. Hong Kong University of Science and Technology Research Center; 1996.

[26] Inaudi JA. Modulated homogeneous friction: a semi-active damping strategy. Earthq Eng Struct Dyn 1997;26(3):361–76.

[27] Spencer BF, Dyke SJ, Sain MK, Carlson JD. Phenomenological model of a magnetor-heological damper. J Eng Mech 1997;123(3):230–8.

[28] Symans MD, Kelly SW. Fuzzy logic control of bridge structures using intelli- gent semi-active seismic isolation systems. Earthq Eng Struct Dyn 1999;28: 37–60.

[29] Choi KM, Cho SW, Jung HJ, Lees IW. Semi-active fuzzy control for seismic response reduction using magnetorheological dampers. Earthq Eng Struct Dyn 2004;33(6):723–36.

[30] Kim HS, Roschke PN, Lin PY, Loh CH. Neuro-fuzzy model of hybrid semi-active base isolation system with FPS bearings and an MR damper. Eng Struct 2006; 28:947–58.

[31] Zbikowski R, Hunt KJ. Neural adaptive control technology. World scientific series in robotics and intelligent systems, Vol. 15. Singapore: World Scientific; 1996.

[32] Narasimhan S, Nagarajaiah S, Johnson EA, Gavin HP. Smart base-isolated benchmark building. Part I: problem definition. Sruct. Control Health Monit 2006;13:573:588